Evaluation of Past and Projected Climate Change in Pakistan Region Based on GCM20 and RegCM4.3 Outputs

Ahmad, B.[1], A. Hussain[2]

Abstract

Attributes of climate change in Pakistan using high resolution outputs from a General Circulation Model (GCM) viz. GCM20 and from a Regional Climate Model (RCM) viz. RegCM4.3 are presented in this paper. Recently published reanalysis dataset AgMERRA is used as standard observation over the country. Scenarios induced (A1B under AR4 and RCP8.5 under AR5) spatial changes in 2008-2025 and 2080-2098 projection periods as compared to 1980-1998 baseline period are presented. It is seen through the results that under A1B scenario GCM20 mean DJF temperature change in 2008–2025 projection period suggests an up to 5°C rise in the North–most region of the country. GCM20 JJAS precipitation rate of change under A1B scenario in the 2008–2025 projection period suggests a relative decrease of up to 20 mm/day over the central parts of the country. RegCM4.3 under RCP8.5 scenario suggests an up to 11°C rise in the mean temperature projection of 2008–2025 DJF season over the Northern region of the country. Moreover RegCM4.3 under RCP8.5 suggests a mean JJAS precipitation decrease of up to 0.5 mm/day in 2008–2025 projection over South–eastern region of the country. The regional forcing, internal dynamic of the models and high level of uncertainties in the observational–based climate dataset could undermine the confidence on the future projection as well as the mitigation and adaptation strategies under a changing climate.

Key Words: Pakistan region; AgMERRA; GCM20; RegCM4.3; A1B; RCP8.5; Seasonal climate change

Introduction

Upon the investigation of past climate, robust change has been illustrated in Pakistan (Farooqi et al., 2005). The pace and attributes of climate change has differed over space and time throughout the country. Necessary engagements in efforts to reduce impacts of Green House Gases (GHGs) in the atmosphere has catered for adaptation measures in perspective of changing climate. Literature provides enough evidence for future changes in the climate - owing to which the water resources, the food sector, health industry, transportation and sustainability of the ecosystem has already taken its toll on the country. It has largely been suggested to employ adaptation programs to survive emanating risks posed by climate change to the agriculture and water resources sector in Pakistan (Janjua et al., 2010 and Rasul et al., 2012).

Present era experiences climate change hazards never heeded before by humankind. Anthropogenic activity has deteriorated this experience to an extent of no return. Agriculture being one of the prime sector to human sustainability is a considerable sufferer. Pakistan is an agricultural country which has nearly 47% of its society attached to this sector. Large concentrations of GHG emissions have rendered temperatures soaring and precipitation patterns diminishing globally. Impacts of climate change induce serious threats to the agrarian economy of Pakistan (Shakoor et al. 2011). Food security is now negatively impacted through abrupt temperature variations in the region. In particular, the Punjab province based farmers are majorly affected whose sole revenue is dependent upon crop production in arid lands. Although, to some crops the increasing GHG contributes positively, yet the overall measure of pessimistic repercussion of temperature overthrows the appreciative response of GHGs in the region.

Rouf et al. (2011) and Mizuta et al. (2012) began the analysis to verify the capability of a super high resolution GCM – GCM20 (20–km horizontal resolution) over South Asian regions. Their studies focused the Indian and Bengal regions to which the model performed decent enough to reproduce the sudden onset

[1] burhanahmadkhan@gmail.com, R& D Division, Pakistan Meteorological Department, Pitrus Bukhari Road, Sector H-8/2, Islamabad, Pakistan

[2] Department of Meteorology, COMSATS Institute of Information Technology, Islamabad, Pakistan

and gradual withdrawal of monsoon. Past, present and future climatic patterns (for precipitation and temperature) were assessed over the Northwest and Southwest regions of Bangladesh. To those regions, it was inferred that there exists an increasing trend for temperature (up to 4.34 °C/100 years) and a decreasing trend for the precipitation (up to 1.96mm/100 years). A projection of global warming was carried out using time slice technique for GCM20 (Kusunoki et al., 2006). The model reproduced a realistic Baiu season, northward seasonal march of the Baiu rain band, its onset and withdrawal, intensity of rainfall and the geographic distribution of mean sea level pressure. To evaluate the dependency of the reproducibility of the Baiu rain band over the horizontal resolution, experiments were carried out that revealed relatively higher performance of 20-km model over the lower horizontal resolution models. Future projections of the precipitation showed an intensity increase over the Yangtze River valley of China, the East China Sea, Western Japan, and the ocean to the south of the Japan archipelago, with an intensity decrease over the Korean Peninsula and Northern Japan.

The Coordinated Regional Climate Downscaling Experiment (CORDEX) is a foundation drafted to integrate international attempts made on simulation of regional climate under domains that surround major land areas of the world (Ozturk et al., 2012). The International Centre for Theoretical Physics (ICTP) RCM named RegCM 4.0, a contributor to the CORDEX project, has been widely brought to play owing to its enclosure of land surface, air-sea flux schemes, planetary boundary layer (PBL), an assorted convection and tropical band configuration, under several CORDEX domains (Giorgi et al., 2012). Over Central Asia, a baseline simulation from 1989-2010 using ERA-Interim reanalysis data as the boundary condition, a baseline simulation from 1970-2010 using a GCM ECHAM5 data under A1B scenario as boundary forcing, and a projected simulation for the period 2070-2100 using the GCM ECHAM5 as the forcing data, has been performed to study future trends of temperature and precipitation (Ozturk et al., 2012). Despite of heterogeneous terrain of the region, RegCM4.0 was successful in capturing the effects of Indian Monsoon system, in addition to the general climatic features of the region.

In view of the quality of mimicking studied physical phenomena as cited above for GCM20 and RegCM4, the considered models seems to be well suited for Pakistan. The country bears an agricultural based economy and therefore demands vital knowledge of the changes in spatial distributions of the basic climatic fields. In this context, time averaged spatial maps of temperature and precipitation on seasonal basis are presented in this paper to assess changes in spatial distributions of climate over Pakistan.

Data and Methodology

Data

Baseline Reanalysis Dataset AgMERRA

Under the present work, spatial analysis of state of the art newly published Agricultural Modern Era Retrospective Analysis for Research and Applications (AgMERRA) datasets (Ruane et al., 2014) for temperature and precipitation is carried out on country level for baseline period (1980-1998). The dataset has been developed from the previously established Modern Era Retrospective Analysis for Research and Applications (MERRA) incorporated with in situ and satellite sensed observational datasets for temperature, precipitation and other important meteorological variables. The AgMERRA introduces daily high resolution climate forcing datasets for the period 1980-2010 to study climate variability and climate change impacts in addition to their use in agriculture sector. The AgMERRA incorporates Hadley Integrated Surface Dataset (Dunn et al., 2012) which comprises several accepted climate stations of the Pakistan region that compares and correlates well with in-situ observations (Ruane et al., 2014).

Baseline and Projected GCM20 Dataset

Present research work has utilized the output from global 20–km mesh model, GCM20 – a collaborative development of Japan Meteorological Agency (JMA) and the Meteorological Research Institute (MRI). The model has a linear Gaussian grid that triangularly truncates at 959 horizontal units. The model is based on operational numerical weather prediction model of JMA, and assimilates modifications in radiation and land surface processes (Mizuta et al., 2012). The model had been simulated with a time step of 6 minutes, and is capable of providing data at 60 vertical pressure levels (1000 hPa – 0.1 hPa). The grid size of the model is 1843200 units with a grid resolution of 1920×960. The model simulation had been performed under A1B scenario in 3 time slices: 1980–1998, 2007–2025, and 2080–2098 (Table 1).

Baseline and Projected RegCM4.3 CORDEX Dataset

RegCM4.3 CORDEX South Asia from Center of Climate Change Research (CCCR) (http://cccr.tropmet.res.in/home/models_data.jsp) is newly published, fourth generation development of ICTP based RCM (Giorgi et al., 2012). It is a hydrostatic model with sigma–p vertical coordinates, and is run on an Arakawa B–grid. The model has a capacity to incorporate various reanalysis datasets, GCM outputs, and CMIP5 model outputs, as its boundary conditions. The simulation period of the experimental design starts from 1st Jan 1970 to 31st Dec 2099, which captures both the baseline and the projection periods. The initial and boundary conditions for the model came from CMIP5 based GFDL–ESM2M (RCP8.5) with 2.0°×2.5° spatial resolution. The radiation scheme used in the simulation was taken from NCAR based CCM3. Biosphere–Atmosphere Transfer Scheme (BATS) had been used in Land surface physics. Planetary boundary layer parameterization had been done using Holtslag's scheme. The convective precipitation scheme has been taken over land by Emanuel, and over ocean by Grell with Fritsch–Chappel as the closure scheme. Large–scale precipitation scheme was based on Subgrid Explicit Moisture Scheme (SUBEX), while ocean flux parameterization had come from Zeng's scheme (Ozturk et al., 2012 and Hassan et al., 2014). Exponential relaxation of 20 grid points width were selected for lateral buffer zone in order to address lateral boundary treatment in the model.

Table 1: Datasets, period and variables availability for analysis.

Dataset/Model	Available Period	Variables	Spatial Resolution	Time step	Scenario
AgMERRA	1981–2010	Temperature, Precipitation	25 km	Daily	–
GCM20	1979–1998	Temperature, Precipitation	20 km	Monthly	A1B
	2007–2025				
	2080–2098				
RegCM4.3	1970–2099	Temperature, Precipitation	25 km	3 hourly	RCP8.5

Out of several CMIP5 GCMs, the present study has chosen to use the version of RegCM4.3 forced with the GFDL-ESM2M boundary conditions owing to their dominant abilities in emulating South Asian climate with modest robustness. Ashfaq et al. (2015), for their climate change assessment study over Pakistan region, selected the GFDL-ESM2M GCM based on several facts such as the track record of publications, better performance in monsoon regions and reputation of the model developing institute. RegCM4.3 forced with GFDL-ESM2M has shown the ability to adequately capture the precipitation patterns and its magnitude over the Northern domain of Pakistan (Hassan et al., 2014 and Burhan et al., 2015). Moreover the boundary forcings induced by the GFDL-ESM2M in RegCM4.3 indicated that South Asian summer monsoon mean temperature change is consistent with clear projection of warming (Hassan et al., 2015). Furthermore climatology of South Asian summer monsoon precipitation and low level westerlies for the historical period are well represented by the GFDL-ESM2M forced RegCM4.3 over the South Asian domain (Mamgain et al., 2013).

Methodology

Extraction of Data at Stations

For the 44 ground stations listed in Figure 1 and Table 2, extraction of daily mean temperature and total precipitation from the AgMERRA dataset is performed. To project statistics of the future climate, mean projected temperature and total projected precipitation from the super high resolution GCM20 and from the state of the art RegCM4.3 are extracted over several ground stations.

The ground station selection includes general siting (urban, rural, snow–cover, agro–climate, latitudinal location, proximity to ocean, reach of monsoon and westerly systems etc.), and topographic setting since these factors can result in much more variability in temperature and precipitation values than differences. Snow cover can have a major impact on temperature change (especially by its freeze and thaw process) in the vicinity of the selected ground station. Keeping in view these dynamics, the ground station density in higher latitudes above 31°N (below 31°N) is 25(19). Zonally, 7 ground stations have been selected in the snow–covered glaciers of the Northern areas, 3 ground stations in the hills of Azad Jammu and Kashmir, 8 ground stations in the hills and plains of Khyber Pakhtunkhwa, 11 ground stations in the plains of Punjab, 6 ground stations in the deserts and ocean bordering plains of Sindh, and 9 ground stations in the barren hills and coastal line of Baluchistan.

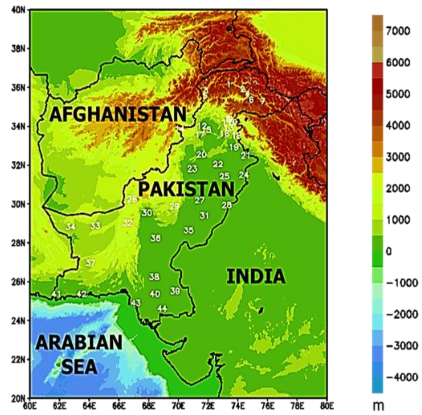

Figure 1: Relief map of study area. Elevation is represented in meters. Station network distribution of the study area is also represented by corresponding serial numbers.

Table 2: Stations with their corresponding coordinates locations and elevations. The stations are arranged in a latitudinal decreasing fashion.

Sr. No.	Station Name	Latitude (°N)	Longitude (°E)	Elevation (m)	Sr. No.	Station Name	Latitude (°N)	Longitude (°E)	Elevation (m)
1	Gupis	36.17	73.40	4682	23	Dera Ismail Khan	31.82	70.92	174
2	Gilgit	35.92	74.33	1469	24	Lahore	31.50	74.40	216
3	Chitral	35.85	71.83	3049	25	Faisalabad	31.43	73.10	185
4	Bunji	35.67	74.63	1340	26	Quetta	30.25	66.88	1571
5	Drosh	35.57	71.78	1666	27	Multan	30.20	71.43	124
6	Astore	35.37	74.90	2945	28	Bahawalnagar	29.95	73.25	157
7	Skardu	35.30	75.68	2211	29	Barkhan	29.88	69.72	1114
8	Balakot	34.38	73.35	1188	30	Sibbi	29.55	67.88	139
9	Muzaffarabad	34.37	73.48	905	31	Bahawalpur	29.40	71.78	126
10	Ghari Dupatta	34.22	73.62	831	32	Kalat	29.03	66.58	2016
11	Kakul	34.18	73.25	1227	33	Dalbandin	28.88	64.40	848
12	Peshawar	34.02	71.58	323	34	Nokkundi	28.82	62.75	677
13	Murree	33.92	73.38	1658	35	Khanpur	28.65	70.68	92
14	Parachinar	33.87	70.08	1592	36	Jaccobabad	28.25	68.47	56
15	Cherat	33.82	71.88	1222	37	Panjgur	26.97	64.10	985
16	Islamabad	33.62	73.10	507	38	Nawabshah	26.25	68.37	29
17	Kohat	33.57	71.43	501	39	Chhor	25.52	69.78	3
18	Kotli	33.52	73.90	608	40	Hyderabad	25.38	68.42	24
19	Jhelum	32.93	73.72	232	41	Jiwani	25.37	61.80	15
20	Mianwali	32.55	71.55	208	42	Pasni	25.37	63.48	15
21	Sialkot	32.50	74.53	253	43	Karachi	24.90	67.13	26
22	Sargodha	32.05	72.67	191	44	Badin	24.63	68.90	10

Bias Correction Using Delta Method

Bias correction based on 'delta method' is done for both the GCM and the RCM in order to project robust temperature and precipitation trends for the 21st century in Pakistan. Delta method or more commonly the 'change factor' method of bias correction for future distributions uses the observed climatological values altered by an adjustment factor. To find adjustment factors for average temperature, our approach is to subtract from individual grids, the GCM–simulated average temperature for a reference period from that for a future period, and for precipitation, the approach is to compute the ratio of the projected future average precipitation to the reference average precipitation (Minville et al., 2008; Tisseuil et al., 2010; Winkler et al., 2011; Chen et al., 2011).

Temporal Disaggregation

Temporal disaggregation of GCM20 (from monthly to daily) and temporal aggregation of RegCM4.3 (from 3 hourly to daily) had been performed to synchronize the temporal resolutions of the models' output into daily format (Salathe 2004). In temporal disaggregation technique, diurnal variations from a projection month are imposed upon all grids of the extracted monthly values. To disaggregate precipitation parameter, daily climatology of the AgMERRA data had been acquired for each grid and then calibrated in a model such that the monthly total precipitation gets equal to the model extracted precipitation total for the corrected month. For temperature, the temporal disaggregation had been executed by employing the same methodology, except for that the calibration was multiplicative rather than additive.

For precipitation, the spatially interpolated grid obtained is temporally disaggregated to daily sequences since it can project diurnal variations in the projected data series. The technique used here is a protraction of that used by Wood et al. (2004), where daily sequences are retrieved by employing monthly means of daily time series instead of picking a random month from the observational records on account that the selection of an arbitrary month may possibly generate incomparable outputs. The diurnal variation harnessed from that month is levied upon all grids of the downscaled monthly values whilst retaining the downscaled monthly mean intact. To disaggregate precipitation parameter, daily climatology of the baseline AgMERRA data is obtained for each grid and then scaled in a model such that the monthly total precipitation gets equal to the downscaled precipitation total for the corrected month as represented in Equation (1) and Equation (2).

$$y_k^{td} = c_j x_i \tag{1}$$

$$c_j = \frac{y_{j\,(proj)}}{\sum_i x_{i\,(ref)}} \tag{2}$$

Where y_k^{td} is the temporally disaggregated daily precipitation time series, c_j is the scaling factor, x_i is the reference day from the climatology month, $\sum_i x_{i\,(ref)}$ is the monthly sum of x_i and $y_{j\,(proj)}$ is the spatially bias corrected monthly precipitation total. This provides us the daily sequence of projected daily precipitation time series superimposed with the daily signal from the baseline dataset.

For temperature, the temporal disaggregation is carried out using the same methodology as is done for precipitation with the exception that the adjustment factor is added (Equation (3)) instead of being multiplied. The reference sequence of daily mean temperature is recalibrated by a constant factor d_j such that the monthly average of the altered daily mean temperature gets equal to the bias corrected monthly temperature value over the projections as represented in Equation (4).

$$\beta_k^{td} = d_j + r_i \tag{3}$$

$$d_j = w_{j\,(proj)} - \bar{r}_{i\,(ref)} \tag{4}$$

Where β_k^{td} is the temporally disaggregated daily temperature time series, d_j is the temperature adjustment factor, r_i is the reference day form the climatology month, $w_{j\,(proj)}$ is the spatially downscaled monthly temperature value and $\bar{r}_{i\,(ref)}$ is the monthly average of r_i. The final output is a daily bias corrected temperature and precipitation data series ready to be used for projection analysis.

Results and Discussion

Analysis Architecture

Seasonal analysis over Pakistan is done for daily mean temperature and precipitation for baseline period (1980–1998) and two projected periods (2008–2025 and 2080–2098) by constructing their spatial gradient maps in order to identify possible climate change signatures in the region. Daily temperature and precipitation is first categorized into 4 seasons (DJF, MAM, JJAS and ON) and then time-averaged over the entire periods length.

AgMERRA Based Seasonal Changes

Spatial distribution of AgMERRA seasonal mean temperature is represented in Figure 2. Mean temperature variation from North to South of the country is evident in all seasons by the AgMERRA dataset. Extreme North of the country experiences a relative cold climate whose mean temperature drops to –15°C in the DJF season and goes up to 15°C in JJAS season. In the MAM and ON transitional periods of Pakistan, AgMERRA has illustrated sub–zero temperature ranges (–5°C to –10°C) in the extreme North regions of the country. The retention of sub–zero mean temperature in the North of Pakistan is due to the glaciated region of the country whose climate is majorly affected by terrain height, Tibetan High, Siberian High and Westerly winds systems.

The Northeast region of Pakistan exhibits a variable climate amongst the seasons. AgMERRA depicts coldest mean temperature range (15°C to 20°C) in DJF season whilst it depicts the warmest mean temperature range (30°C to 35°C) in the JJAS season. In the MAM season, AgMERRA has shown a mean temperature range of 25°C to 30°C, whereas, in the ON season, it has shown a mean temperature range of 20°C to 25°C, in the Northeast region of the country. An extensive portion of the Northeast region of Pakistan is planar with larger surface area to absorb incoming shortwave radiation. This makes the Northeast region prone to temperature related calamities, especially in the JJAS season.

The Northwest region of the country circumscribes trails of Hindukush with ice–covered peaks, owing to which mean seasonal temperature change has significant adverse effects like triggering of Glacier Lake Outburst Flood (GLOF) events (Din et al., 2014). As per AgMERRA output, mean temperature in DJF spatially varies from –10°C to 15°C in the Northwest region of the country. Highest spatial variation in mean temperature is observed in JJAS season with a range of 30°C to 10°C in the region. Both MAM and ON seasons show a mean temperature spatial variation of 20°C to –5°C in the Northwest region of the country.

The Southeast region of Pakistan is located along the tropical belt and therefore is prone to hazards like droughts, floods and tropical cyclones. AgMERRA depicts 20°C to 25°C mean temperature retention in DJF season, 25°C to 30°C mean temperature retention in MAM season, 30°C to 35°C mean temperature retention in JJAS season, and 20°C to 30°C mean temperature retention in the ON season of the Northeast region of the country. Seasonal temperature variations bring great catastrophes to this region including droughts and floods in JJAS season, and tropical cyclones in MAM season.

The Southwest region of Pakistan comprises of a heterogeneous terrain with mountains peaking to 2000 m.a.s.l.. Spatial as well as seasonal variation is evident in the region as depicted by AgMERRA daily mean temperature data. Mean temperature spatially varies between 5°C and 25°C in DJF season, between 10°C and 30°C in MAM season, between 20°C and 35°C in JJAS season, and between 10°C and 30°C in ON season. The Southwest region of the country is prone to fresh water scarcity due to its rocky surface and consequently high evapotranspiration and runoff that are direct attributes of variation in temperature regime of the region. Moreover, contrasts in cold advection from the Siberian winds/Shamal winds and the temperature borne warm rocky surface bring dust storms which cause major disasters in the region.

Precipitation patterns have been shown to vary both in space and magnitude upon seasonal analysis of the AgMERRA daily precipitation data. AgMERRA shows mean precipitation intensity of 1 mm/day to 2 mm/day in the DJF season of the Northern belt of the country as represented in Figure 3. The precipitation in this region and season is mostly comprised of snow precipitation since high peaks of HKH region are directly influenced by Jet streams. The MAM season brings more moisture through westerly winds with broader spatial extent towards the Northwest region of the country. The magnitude of mean precipitation along the Westerly belt in MAM season is up to 5 mm/day as shown by AgMERRA data.

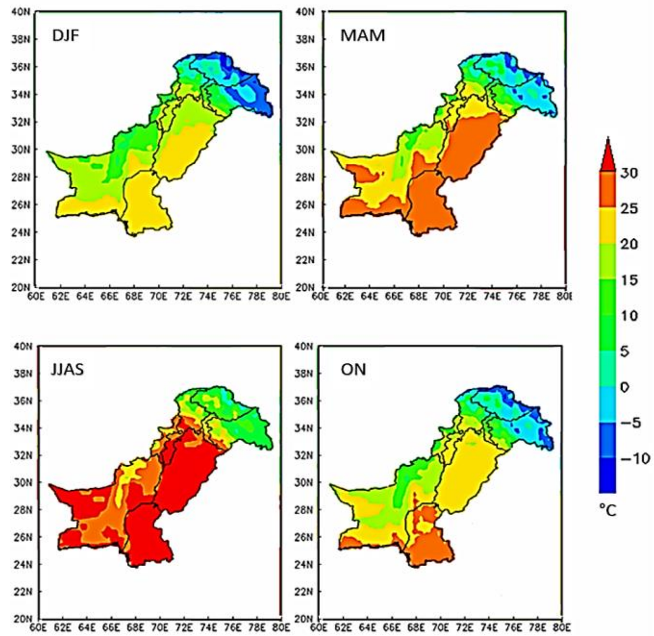

Figure 2: Spatial distribution of mean seasonal temperature (°C) by AgMERRA for baseline period 1980–1998.

Summer season (JJAS) in Pakistan bring monsoon precipitations to Northern, North–eastern, North–western, and South–eastern parts of the country. AgMERRA shows 6 mm/day to 7 mm/day mean precipitation in the Northeast region, while it shows 2 mm/day to 3 mm/day mean precipitation in the Southeast region of the country. The intrusion of Monsoon and its interaction with Western disturbances can also be observed in the North–western parts of the country, where 2 mm/day to 5 mm/day mean precipitation is shown by AgMERRA data. In the ON season, the Monsoon retreats and the Western disturbances begin to take strength with mean precipitation magnitude of 1 mm/day to 2 mm/day in the Northwest region of the country, as depicted by AgMERRA precipitation data.

Temporally averaged extremes of mean temperature (°C) and mean precipitation (mm/day) for AgMERRA are summarized in Table 3.

Table 3: Extremes of mean temperature (°C) and precipitation (mm/day) figures for AgMERRA over Pakistan.

AgMERRA			
Time Scale	**Season**	**Temperature (°C)**	**Precipitation (mm/day)**
1981-1998	DJF	-15(25)	2
	MAM	-10(30)	5
	JJAS	-5(35)	7
	ON	-15(30)	2

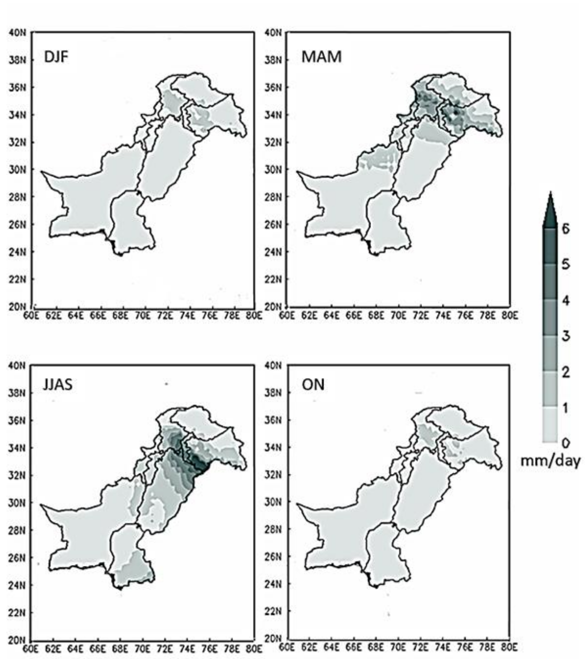

Figure 3: Spatial distribution of mean seasonal precipitation (mm/day) by AgMERRA for baseline period 1980–1998.

GCM20 Based Seasonal Changes

Model based historical run of GCM20 has been analysed on seasonal basis to assess spatial variations over the country. The A1B scenario under which the GCM20 has been simulated heralds a balance between the use of fossil intensive and non–fossil energy resources by the end of century. Seasonal analysis of GCM20 historical run suggests a retention of sub–zero mean temperatures (down to –18°C) in the DJF season over the Northern regions of the country as represented in Figure 4. In the same season, North–eastern side shows a spatial temperature range of 6°C to 18°C which on comparison with the observed AgMERRA dataset suffers from a 7°C mean temperature cold bias. The DJF mean temperature range represented by GCM20 in the North–western side varies from 0°C to 18°C which on comparison with AgMERRA dataset is in good spatial accordance. The South–most side of the country which harbors ocean to Arabian Sea depicts a mean temperature range of 12°C to 24°C, as simulated by GCM20 temperature data.

The historical run of GCM20 has shown cold biases in MAM season. The extreme North region of the country depicts a mean temperature range of –18°C to 0°C, as seen through the GCM20 temperature data, which is 3°C colder than the observed AgMERRA temperature dataset. The North–eastern region of the country illustrates a mean temperature range of 12°C to 18°C as simulated by GCM20 in the MAM season. Towards the South–eastern region, GCM20 depicts an 18°C to 24°C mean temperature range in the MAM season. The North–western region of the country bears a mean MAM temperature range of 6°C to 12°C as illustrated by GCM20. Moreover, GCM20 in the South–western region of the country depicts a spatial distribution of mean temperature range between 6°C to 24°C which is 1°C colder than that depicted by observed AgMERRA dataset.

Mean temperature patterns simulated by GCM20 in the JJAS season are in good compliance with the observed AgMERRA dataset, though with a few warm biases in the North. The North–most region of the country shows a temperature range of 6°C to 12°C mean temperature range, as simulated by GCM20, which is 2°C warmer than that seen by observed AgMERRA dataset in the JJAS season. Towards the North–eastern side, the mean temperature range varies spatially from 24°C to 36°C in the JJAS season. GCM20 shows agreeable mean temperature range of 30°C to 36°C with the observed

AgMERRA dataset, in the JJAS season of the South–eastern region of the country. Moreover, GCM20 shows agreeable mean temperature ranges of 18°C to 30°C in the North–western region, and of 24°C to 36°C in the JJAS season of South–western region of the country.

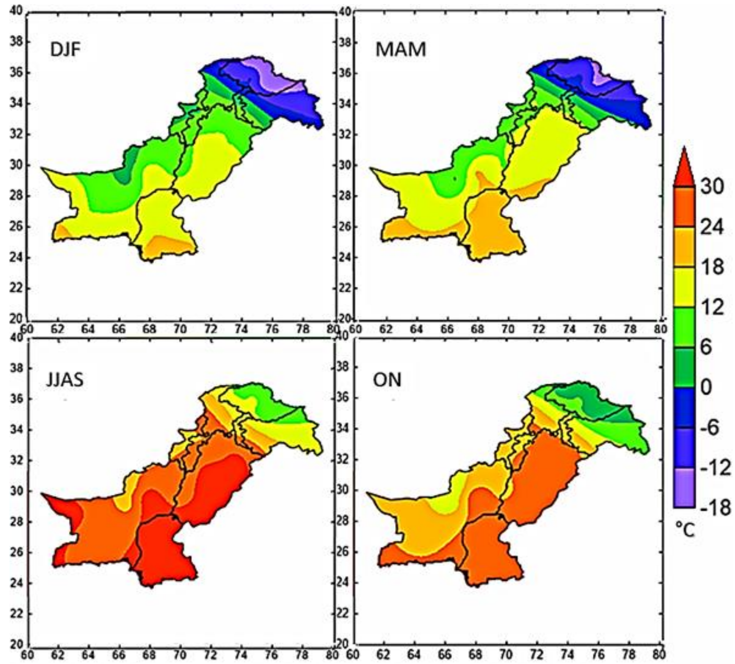

Figure 4: Spatial distribution of mean seasonal temperature (°C) simulated by GCM20 for baseline period 1980–1998.

The simulation of mean temperature in ON season by GCM20 shows 3°C warm bias in the North–most region of the country. Towards the North–eastern and the South–eastern sides of the country, GCM20 simulates 24°C to 30°C mean temperature range, which is 4°C warmer as compared to that illustrated by observed AgMERRA dataset in the ON season. Moreover, the South–western side of the country shows a mean temperature range of 12°C to 30°C in the ON season which suffers from a 2°C cold bias with reference to the observed AgMERRA dataset.

Simulation of precipitation over rugged terrains like that featured in Northern and North–western regions of Pakistan is a formidable job. The high spatial resolution of GCM20 has been expected to simulate patterns and magnitude of precipitation that are closest to that observed in AgMERRA precipitation dataset. Seasonal precipitation analysis of GCM20 has revealed concentration of DJF precipitation to the Northern side of the country which is spatially homogeneous to the observed AgMERRA precipitation dataset as seen through Figure 5. Mean precipitation simulated by GCM20 in the DJF season ranges between 4 mm/day to 10 mm/day in the North–eastern and the North–western regions of the country. In the MAM season, GCM20 simulates 7 mm/day to 11 mm/day mean precipitation in the North–eastern region, while it simulates a 1 mm/day to 6 mm/day mean precipitation in the South–eastern region of the country. The GCM20 has realistically simulated the precipitation patterns resulting from western disturbances in both DJF and MAM seasons. However magnitude of the mean precipitation is overestimated by 2 mm/day in the DJF season and by 4 mm/day in the MAM season towards the North side of the country. Moreover, the precipitation intensity towards the South–eastern side simulated by GCM20 has resulted in wet bias of up to 3 mm/day in the MAM season. The MAM season in Pakistan is a transitional period with tropical cyclone occurrences in the Arabian Sea. Possible explanation for wet bias in the South–eastern region of the country might be the precipitation resulting from these cyclones in the MAM season.

Simulation of JJAS mean precipitation by GCM20 results in a spatial dislocation of the high intensity precipitation belt as observed in AgMERRA precipitation dataset. The central part of the country receives the highest amount (exceeding 10 mm/day) of mean precipitation as simulated by GCM20. The observed dataset AgMERRA, however, shows the highest precipitation intensity over North–eastern side of the country in the JJAS season. Previous studies have reported that tropical intraseasonal variability such as the Madden-Julian Oscillation (MJO) in the GCM20 was not so realistic owing to which the model simulated low amplitudes in convection and low level winds in the 30–60 day band oscillations (Mizuta et al., 2012). The GCM20 realistically simulates mean precipitation intensity in the JJAS season towards the South–eastern side of the country with values between 1 mm/day to 3 mm/day which are quite comparable to the AgMERRA mean precipitation in the JJAS season. This attributes to the reproducibility of convective rainfall and associated precipitation improvement by introducing parameterization in cumulus convection in GCM20 (Tatsumi et al., 2013). Moreover GCM20 mean precipitation of 1 mm/day to 2 mm/day in the ON season also compares well with that of the AgMERRA precipitation dataset in the ON season.

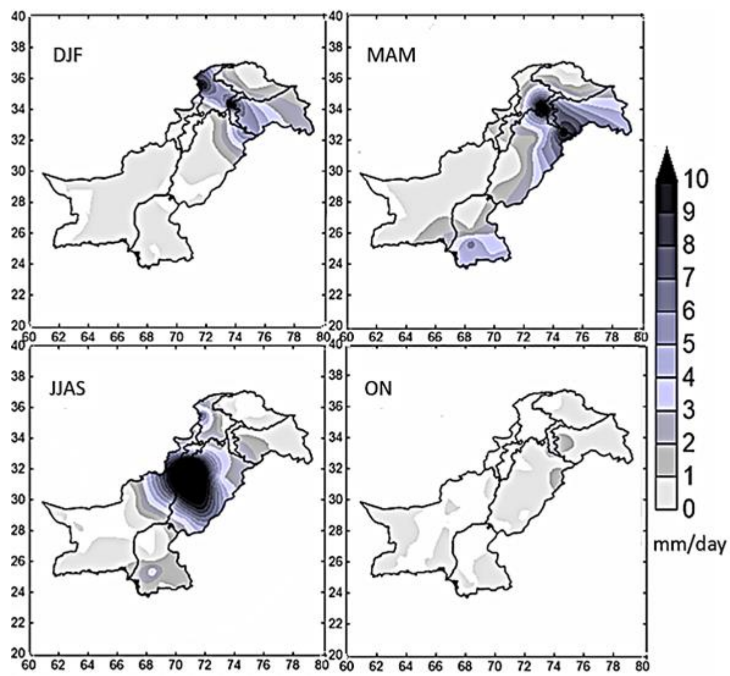

Figure 5: Spatial distribution of mean seasonal precipitation (mm/day) simulated by GCM20 for baseline period 1980–1998.

Near–term mean temperature change through seasons is well evident through GCM20 seasonal projected changes over the country as represented by Figure 6. The present simulation of GCM20 had been done keeping in view the A1B scenario protocols. The A1B scenario represents a balance between the use of fossil and non–fossil fuels. Mean temperature change in the seasons therefore reflects these protocols in their respective projections.

GCM20 mean DJF temperature change in the near future suggests an up to 5°C rise in the North–most region of the country. Moreover, a mean temperature change of up to 3°C has been projected by GCM20 in the near–term future, over the North–western and North–eastern regions of the country. Relatively higher projected changes in the near–future term over the North–most region of the country in the DJF season may possibly be due to the fact that the region is mostly comprised of debris covered glaciers. This renders low albedo values and high absorption rate of incoming solar radiation, hence giving premise to rapid snow melt in the near future period.

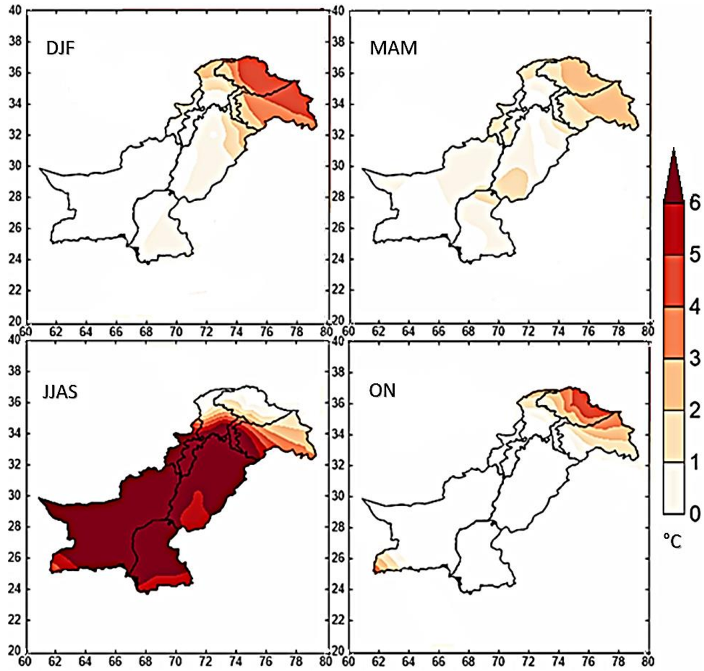

Figure 6: Projected changes (2007–2025 minus 1980–1998) in mean seasonal temperature (°C) simulated by GCM20.

The MAM season mean temperature change in the near–term future suggests an up to 3°C rise in the North–most region of the country. Towards the North–eastern and the North–western regions, the MAM near–term mean temperature change is projected as up to 2°C over the country. In the JJAS season, the GCM20 mean temperature change in the near–term future suggests an up to 4°C rise in the Northern region of the country. Towards the North–eastern and the South–eastern regions of the country, GCM20 suggests a mean temperature increase of 6°C to 7°C in the near–term future projection of JJAS season. The mean JJAS temperature increase (up to 5°C) in the near–term future along the coastal line is smaller than its adjacent landlocked region probably owing to its exposure to sea breeze (due to land–ocean temperature gradient) in the season. In the ON season, North–most part of the country has been projected with almost 5°C rise in the mean temperature of near–term future. In addition, an up to 4°C rise in the mean temperature, along the coastal belt of the South–eastern region of the country is also evident in the ON season of the near–term future period.

Near–term mean precipitation changes in the GCM20 projections show both increase and decrease in the intensity over different seasons as seen through Figure 7. The DJF mean precipitation has been projected to increase by 20 mm/day in the North–western region, and by 12 mm/day in the South–western region of the country. Both regions which project an intensity increase in the mean DJF precipitation are prone to strong westerly systems. GCM20, therefore, projects an even stronger westerly systems in the DJF season on the near–term future period (Burhan et al., 2014).

The GCM20 mean precipitation projection in MAM season shows up to 12 mm/day decrease in the near–term future over the Northern domain of the country. A decrement of up to 4 mm/day has also been projected by GCM20 in the near–term future mean precipitation over the South–eastern region of the country. The JJAS season in the near–term future projection also show a relative decrease of up to 20 mm/day in the mean precipitation regime over the central part of the country. This shows that under A1B scenario protocols, the near–term future projection of mean precipitation along the monsoonal belt is likely to decrease in the region, as projected by GCM20. Moreover, GCM20 projects no significant change in ON mean precipitation in the near–term future period over Pakistan.

Mean temperature change in far future period projected by GCM20 has a broader spatial extent and a higher magnitude as compared to the near term mean temperature projection of GCM20 over Pakistan as seen through Figure 8. The GCM20 DJF season mean temperature projection in the far future suggests an up to 5°C rise in the North and an up to 4°C rise in the North–eastern part of the country. Towards the South–eastern region, the far future projection of GCM20 show an up to 3°C rise in the DJF season. The significant mean temperature rise towards South–eastern region of the country of the far future period seems to be the result of an increase in the SST adjacent to the coast in the DJF season, since SST climatology over the region suggests a relatively warmer ocean in winters as compared to its adjacent coastal area (Ahrens 2000).

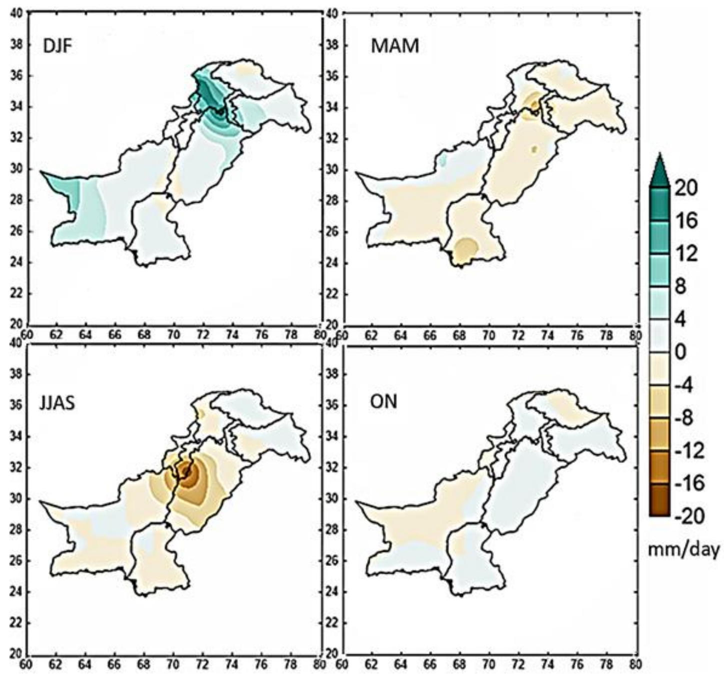

Figure 7: Projected changes (2007–2025 minus 1980–1998) in mean seasonal precipitation (mm/day) simulated by GCM20.

The GCM20 far future projection of mean temperature in the MAM season depicts an 11°C rise in the extreme North of the country. Towards the North–eastern and the South–eastern regions, the mean temperature rise in the MAM season is 6°C to 9°C as projected by GCM20 in the far–future period. The North–western region of the country show high spatial variation in the mean temperature rise (6°C to 11°C) in the far future MAM projection of GCM20. Highest mean temperature rise in the far future JJAS season (up to 11°C) has been shown to occur in the South–western region of the country, as projected by GCM20. The South–eastern side of the country depicts a 4°C to 6°C rise in the JJAS far future mean temperature projection of GCM20. Owing to seasonal intrusion of JJAS monsoon in the North–eastern region of the country, the mean temperature projection show a relatively smaller rise (3°C to 5°C) in the far future period. Towards the North and the North–western side of the of the country, the JJAS mean temperature projection by GCM20 depicts a 3°C to 7°C rise in the far future period. Moreover, the far future MAM season of GCM20 projects a 6°C to 9°C rise in the Northern region, 1°C to 6°C rise in the North–eastern region, 5°C to 6°C rise in the South–eastern region, 3°C to 7°C rise in the South–western region, and 1°C to 6°C rise in the North–western region of the country.

Far future mean precipitation projected by GCM20 illustrates 3 mm/day to 6 mm/day increase over the North and North–eastern regions of the country in the DJF season as shown in Figure 9. The North–western region of the country depicts an up to 15 mm/day mean precipitation rate increase in the far future DJF season, as projected by GCM20. The model also shows that a simultaneous mean precipitation rate increase of up to 12 mm/day is projected in the far future DJF season over the South–

western region of the country. In the far future MAM season, GCM20 projects dryness of down to 12 mm/day in the North–eastern region of the country. Similar drying conditions (of down to 6 mm/day) in the far future are projected by GCM20 in the MAM season over the South–eastern region of the country. On the other hand, GCM20 far future projection in the MAM season over the South–western region suggests an up to 9 mm/day increase in the precipitation rate.

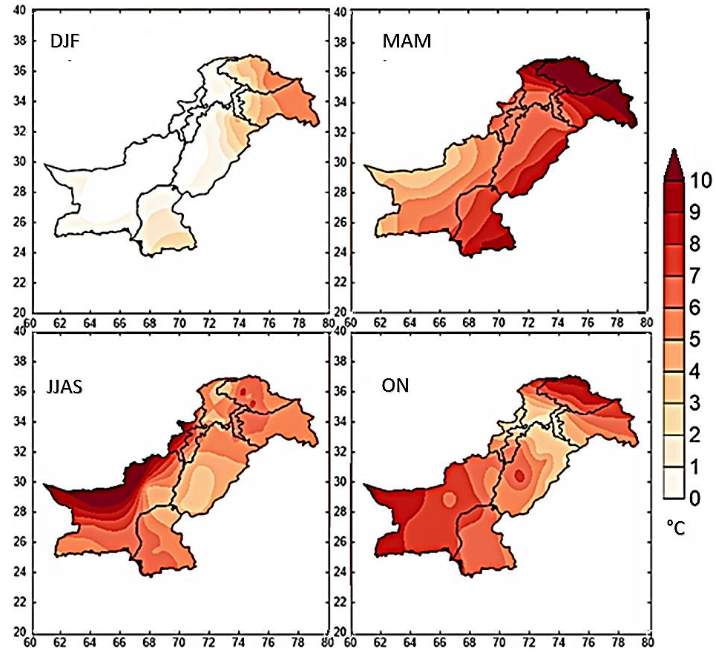

Figure 8: Projected changes (2080–2098 minus 1980–1998) in mean seasonal temperature (°C) simulated by GCM20.

Far future JJAS mean precipitation depicted by GCM20 suggests an up to 15 mm/day increase in the North–eastern as well as in the South–eastern regions of the country. The increase in JJAS mean precipitation is over the regions where monsoon currents reach throughout the season. There is also a

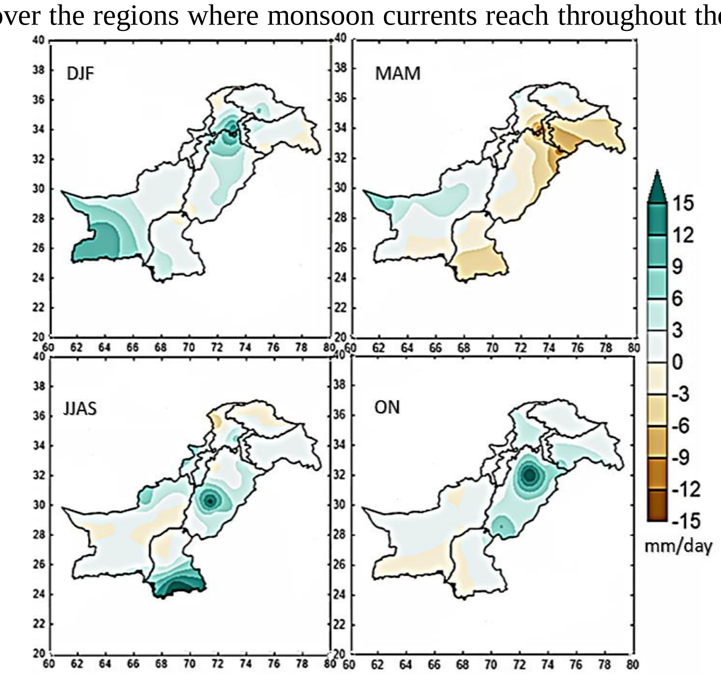

Figure 9: Projected changes (2080–2098 minus 1980–1998) in mean seasonal precipitation (mm/day) simulated by GCM20.

significant mean precipitation increase of up to 6 mm/day in the North–western region of the country in the JJAS season, as projected by GCM20. Moreover GCM20 also projects up to 15 mm/day mean precipitation increase in the far future ON season over the North–eastern region of the country. These significant mean precipitation changes in JJAS and ON season in the far future period produce wetter conditions in contrast to those in the present and near future period which produce relatively drier conditions under the A1B scenario projections over Pakistan.

Previous studies with GCM20 outputs have seen a clear increasing tendency in consecutive and heavy precipitation expectation value for major Pakistani basins in both seasons of MJJAS and NDJFM. At the same time, drought tendency in the Pakistani basins were seen to get strengthened throughout the year in the future yet consecutive dry days decreased in their highland areas contrarily. It suggested that the Pakistani basins might be more sensitive to the projected climate change impact than other basins in the vicinity (Iwami et al., 2017).

Projected changes in temporally averaged extremes of mean temperature (°C) and mean precipitation (mm/day) for GCM20 are summarized in Table 4.

Table 4: Projected changes in temporally averaged extremes of mean temperature (°C) and mean precipitation (mm/day) for GCM20.

GCM20			
Time Scale	**Season**	**Δ Temperature (°C)**	**Δ Precipitation (mm/day)**
2007-2025	DJF	5	24
	MAM	3	-8
	JJAS	7	-20
	ON	5	insignificant
2080-2098	DJF	7	15
	MAM	11	-12
	JJAS	11	18
	ON	10	18

RegCM4.3 Based Seasonal Changes

The Seasonal analysis over mean temperature suggests that RegCM4.3 realistically simulates the seasonal variability at fine spatial scale. There are, however, a few warm and cold biases evident in the seasons (Syed et al., 2014). The RegCM4.3 depicts sub–zero mean temperature ranges (–2°C to –20°C) in DJF and MAM seasons of the North–most regions of the country as represented by Figure 10. AgMERRA on the other hand takes the lower limit of the mean temperature to –15°C in the DJF and MAM seasons of the Northern side of the country. The cold bias of RegCM4 is in line with the previous studies that have also seen tendency of the RegCM4 to underestimate temperatures over the Northwestern Himalaya region (Syed et al., 2014 and Coppola et al., 2014). The North–eastern region of the country illustrates a spatial mean temperature range of 4°C to 16°C in the DJF season and a spatial mean temperature range of 10°C to 16°C in the MAM season, as simulated by RegCM4.3. The model depicts a mean temperature range of 10°C to 16°C in the DJF season, and of 10°C to 22°C in the MAM season towards the South–eastern side of the country. The South–western side of the country depicted a mean spatial temperature range of –2°C to 16°C in the DJF season, and a mean spatial temperature range of –2°C to 22°C in the MAM season. The wide mean spatial temperature range of South–western region of the country is due to the high mountain terrain in the North and low coastal relief in South of the country.

RegCM4.3 mean temperature depiction in JJAS reveals comparable results with the observed AgMERRA dataset. Towards North of the country, the mean temperature in JJAS varies spatially from –2°C to 4°C. The North–western region of the country depicts highly heterogeneous spatial temperature range of –2°C to 34°C in the JJAS season. The model illustrates 28°C to 40°C mean temperature range in the South–western side, and 34°C to 46°C mean temperature range in North–eastern and South–eastern sides of the country in the JJAS season. This illustrates an approximately 5°C mean JJAS temperature warm bias in the RegCM4.3 data when compared with the observed AgMERRA dataset. Attributes to such biases are likely related to the treatment of cloud radiative processes in the modelled schemes (Giorgi et al., 1999). The ON results of RegCM4.3 also displays warm bias in the Northern region of the country. RegCM4.3 estimates mean temperature range of –2°C to 4°C, whilst AgMERRA depicts that between 0°C to –10°C in the JJAS season of the Northern region of the country.

RegCM4.3 illustrates historical mean precipitation accumulated in the Northern and North–western parts of the country during the DJF, MAM and ON seasons, which is spatially homogeneous to that observed in AgMERRA precipitation dataset. Mean precipitation in DJF season over the Northern region of the country ranges from 0.5 mm/day to 2 mm/day as seen in Figure 11. This mean precipitation rate in DJF season has comparable magnitude to that of AgMERRA precipitation dataset, but extends to a larger area in the North. The MAM precipitation in the Northern and North–western sides of the country is well simulated with comparable magnitude of up to 4 mm/day, but with larger extension towards North and smaller extension towards Northwest, as compared to AgMERRA precipitation dataset.

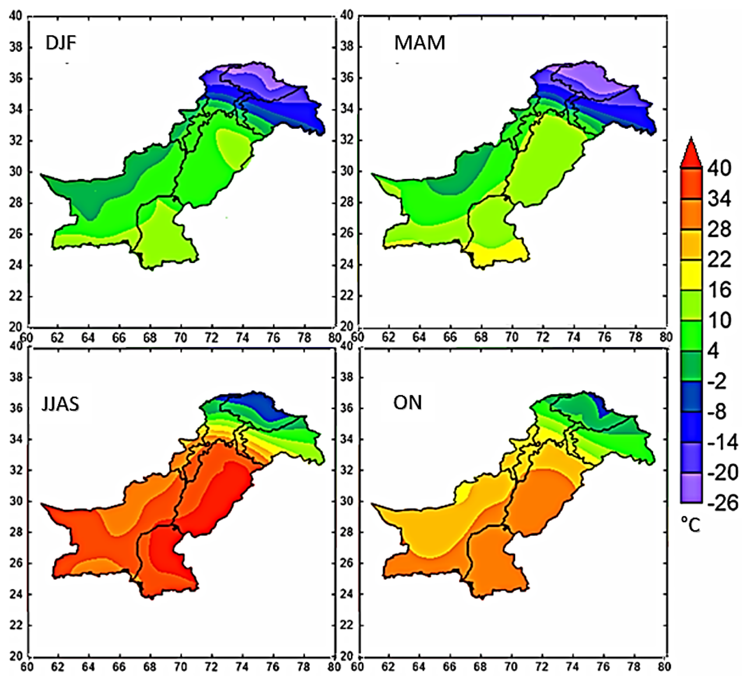

Figure 10: Spatial distribution of mean seasonal temperature (°C) simulated by RegCM4.3 for baseline period 1980–1998.

Simulation output of RegCM4.3 in the JJAS season illustrates a mean precipitation rate of up to 5.5 mm/day along the Northern monsoon belt of the country. AgMERRA mean precipitation in JJAS also depicts the same with analogous mean precipitation rate, but with more southward tilt of the high concentration Northern monsoon belt. Moreover, the RegCM4.3 in JJAS season overestimates mean precipitation in the extreme North of the country, when compared with AgMERRA precipitation dataset. The wet bias attributed to topographically induced strong precipitation pattern is well sensed in RegCM4 (Hassan et al., 2015). Low level jet over the Arabian Sea is one of the significant features of south Asian summer monsoon through which the moisture is transported into the flow of monsoon circulation (Raju et al., 2015). In addition, the moisture transport over the Arabian Sea is considered as the major source of the south Asian summer monsoon precipitation over Pakistan and adjoining regions (Kalim and Gao 2012). Towards the North–eastern side of the country, the JJAS mean precipitation amounts to 2.5 mm/day, as simulated by RegCM4.3, and is comparable to 2.5 mm/day mean precipitation rate in JJAS shown by AgMERRA in the same region. The comparable magnitudes and better spatial patterns of precipitation over complex topography of the domain in the high resolution RegCM4 have also been identified by Hassan et al. (2015). It was hypothesized that the precipitation amount in the RCM was strongly dependent to local dynamical forcing and internal model physics integration and parameterization aspects. The South–western region of the country is shown to depict 1.5 mm/day precipitation rate in JJAS season which is not a prominent feature observed in the AgMERRA mean precipitation in the season. Moreover, the mean precipitation is also overestimated by 1.5 mm/day in the RegCM4.3 when compared with that of the AgMERRA dataset, in the ON season. In literature there are instances of RegCM4 reported to have been suffered with systematic biases over the South Asian region (Gao et al., 2001). Gao et al. (2006), however, also reported that RegCM4.3 reduced temperature and precipitation biases and improved simulation result with respect to the driving GCM GFDL-ESM2M. The biases partially come from the driving data set as well as from the Physics of the model (Hassan et al., 2014).

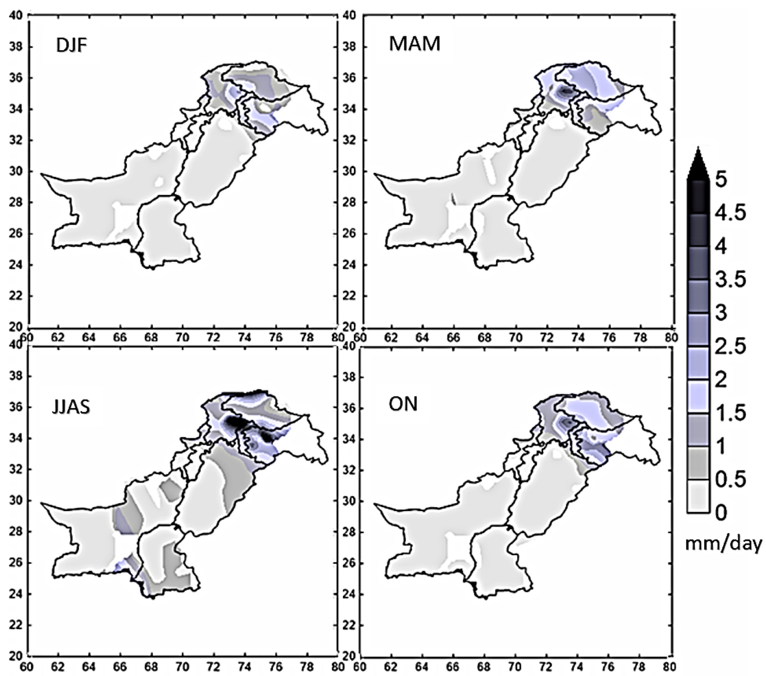

Figure 11: Spatial distribution of mean seasonal precipitation (mm/day) simulated by RegCM4.3 for baseline pe-riod 1980–1998.

RegCM4.3 mean temperature projection in the near term DJF season depicts an up to 11°C rise in the Northern region of the country as represented by Figure 12. Towards the North–western and the North–eastern regions of the country, RegCM4.3 projects up to 9°C rise in the DJF season under RCP8.5 scenario. Moreover, RegCM4.3 also projects up to 10°C rise in the near term DJF season over the extreme South–western region of the country. The MAM season projected by RegCM4.3 RCP8.5 scenario depicts an up to 7°C rise in the near term mean temperature regime over the North–most region of the country. This is followed by a 6°C rise in the MAM mean temperature regime over the South–western region of the country, as projected by RegCM4.3 RCP8.5 scenario.

Mean JJAS temperature projection in the near term future suggests an up to 9°C rise in the North–eastern region of the country, as depicted by RegCM4.3 in RCP8.5 scenario. Towards the South–western region of the country, RegCM4.3 in RCP8.5 projects up to 8°C rise in the near term JJAS season. Both North–western and South–western regions of the country depict an up to 7°C rise in the near term JJAS season, as projected by RegCM4.3 in RCP8.5 scenario. Kumar et al. (2013) and Kazmi et al. (2014) also reported a similar increased tendency in the summer mean surface air temperature over the northern areas of Pakistan, the Himalayas and central India at the end of 21st century. Projected results of near term ON season depict up to 9°C rise in the North and North–eastern regions of the country, as simulated by RegCM4.3 in RCP8.5 scenario. Moreover RCP8.5 scenario depicts an up to 10°C rise in the near term mean ON temperature projection over the South–western region of the country.

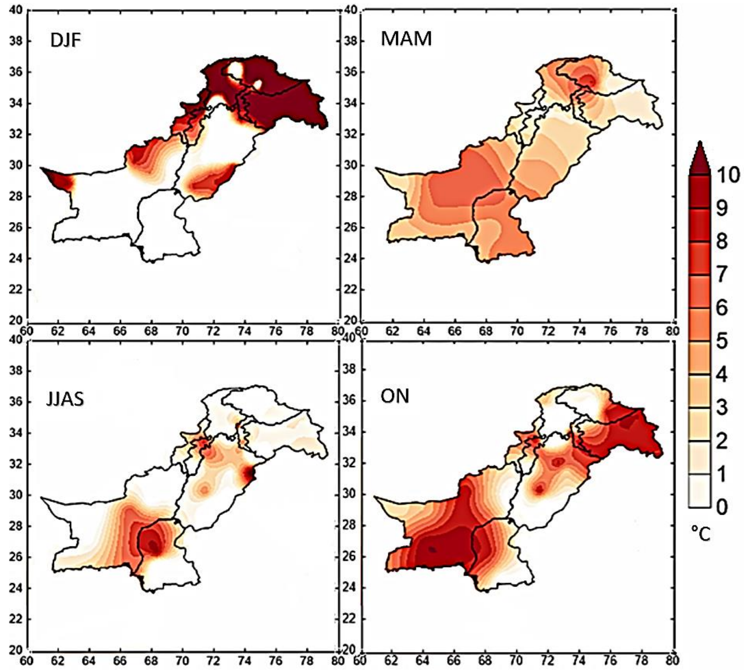

Figure 12: Projected changes (2007–2025 minus 1980–1998) in mean seasonal temperature (°C) simulated by RegCM4.3.

Near term future projection of RegCM4.3 mean DJF precipitation depicts up to 0.6 mm/day increase over the Northern domain of the country as illustrated in Figure 13. Towards the North–eastern region of the country, a mean DJF precipitation decrease of 0.3 mm/day has been projected in the near term future by RegCM4.3. Moreover, the North–western region of the country depicts a mean DJF precipitation decrease of 0.5 mm/day in the near term future projection of RegCM4.3. Furthermore, a mean precipitation increase of up to 0.3 mm/day in the East of South–eastern region, and a mean precipitation decrease of down to 0.3 mm/day in the West of the South–eastern region is also projected in the near term future DJF season.

The MAM season displays combinations of increase and decrease in mean precipitation rates over the near term future projection of the country by RegCM4.3. The extreme North region of the country has been projected with a mean precipitation increase of up to 0.6 mm/day in the MAM season, as projected by RegCM4.3. The Western side of the North depicts a mean precipitation decrease of up to 0.2 mm/day while the Eastern side of the North depicts a mean precipitation increase of up to 0.2 mm/day in the near term MAM future projection of RegCM4.3. A mean MAM precipitation decrease of down to 0.4 mm/day is also projected in the near future by RegCM4.3 over the North–western region of the country.

Relatively drier conditions are depicted in the near term JJAS RegCM4.3 projections. Mean precipitation decrease of down to 0.5 mm/day in near term future are projected in North, North–eastern and North–western regions of the country by RegCM4.3. Moreover, RegCM4.3 also depicts a mean JJAS precipitation decrease of 0.5 mm/day in the near future term over South–eastern region of the country. The decrease in mean JJAS precipitation over the North–eastern and the South–eastern regions of the country reveals that under RCP8.5 protocols, relative strength of Monsoonal currents are expected to get weaker with relatively drier conditions prevailing in the near future period over the country.

The ON season mean precipitation projection in the near term future by RegCM4.3 under RCP8.5 scenario suggests a relative increase throughout the country. Mean ON precipitation increase of up to 0.6 mm/day are projected by RegCM4.3 in the near term future over the Northern region of the country. Towards the North–eastern region, an increase of up to 0.3 mm/day is projected by RegCM4.3 in the near term future projection of the ON season. In addition, an increase of 0.4 mm/day in mean ON precipitation is also projected in the near term future over the South–eastern region of the country. Increase in mean ON precipitation under RCP8.5 over the monsoonal regime signals a delayed withdrawal of monsoon season in the near term future as projected by RegCM4.3.

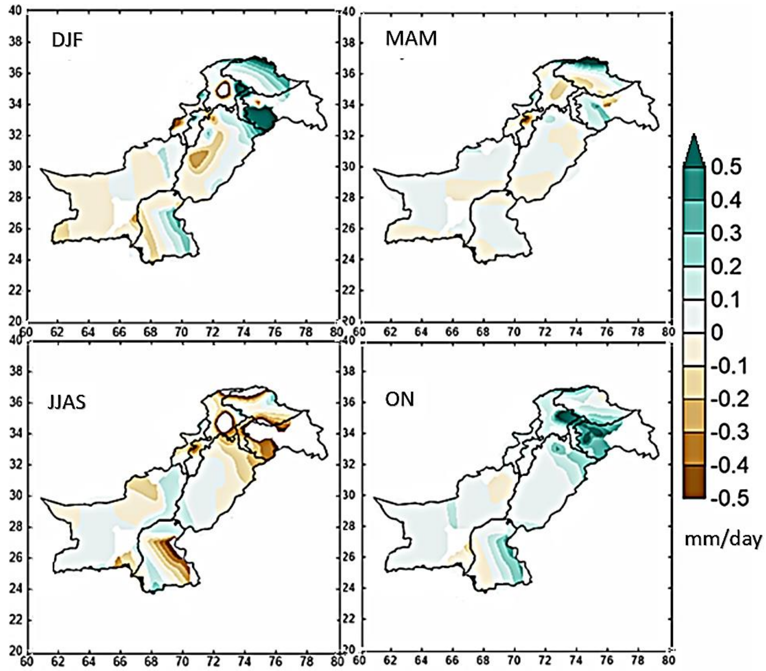

Figure 13: Projected changes (2007–2025 minus 1980–1998) in mean seasonal precipitation (mm/day) simulated by RegCM4.3.

Mean temperature change in the far future as projected by RegCM4.3 under RCP8.5 displays significant rise of up to 11°C as compared to historical period in the Northern region of the country as represented by Figure 14. A 10°C rise has been projected in the DJF season over the North–eastern region of the country in the far future by RegCM4.3. An up to 10°C rise is also projected by RegCM4.3 in the DJF season over the South–eastern and the South–western regions of the country. There is comparatively smaller change in the North–western and in the East of Northern region of the country (rise of up to 4°C). In the MAM season, there is an up to 11°C rise in the far future period over the North of the country, as projected by RegCM4.3. Towards the North–eastern region of the country, a rise of up to 8°C is projected by RegCM4.3 in the far future MAM season. Similar temperature rise of up to 8°C is also projected by RegCM4.3 in the far future MAM season over the North of South–western region of the country. Furthermore, an up to 10°C rise in the West of South–western region, and an up to 11°C rise in the South–eastern region is also projected by RegCM4.3 in the far future MAM season.

Far future projection of RegCM4.3 under RCP8.5 displays relatively smaller spatial extent of change in JJAS mean temperature over the country. The Northern region of the country is projected by RegCM4.3 with an up to 11°C rise in the far future JJAS season. No significant rise in far future JJAS mean temperature is projected by RegCM4.3 over the North–eastern region of the country. Towards the South–eastern region, an up to 8°C rise is projected by RegCM4.3 in the far future JJAS season. Moreover, an up to 7°C rise in the North of South–western region, and an up to 8°C rise in the South of the South–western region is also projected by RegCM4.3 in the far future JJAS season. Our findings for the projected warming over the Pakistani foothills of the Hindukush and Himalayas under RCP8.5

are in–line with the findings of Gu et al. (2006). These warming trends were also predominantly observed over North Pakistan under RCP4.5 and RCP8.5 scenarios by Hassan et al. (2015). Relative spatial span of far future mean temperature rise in ON season is larger as compared to that in JJAS season over the country. The Northern region of the country is projected by a mean temperature rise of up to 11°C rise in the ON far future ON season as projected by RegCM4.3. The North–eastern region of the country depict an up to 8°C rise in the far future ON season as projected by RegCM4.3. Moreover, an up to 10°C rise in the Northern and the Western sides of South–western region is also projected by RegCM4.3 in the far future ON season. Furthermore, an up to 6°C rise in the South–eastern region of the country has also been projected by RegCM4.3 in the far future ON season.

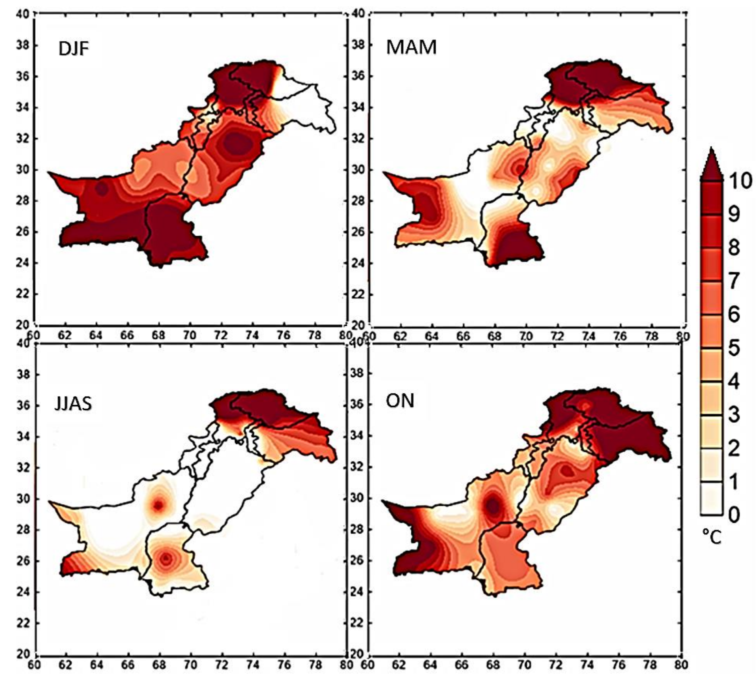

Figure 14: Projected changes (2080–2098 minus 1980–1998) in mean seasonal temperature (°C) simulated by RegCM4.3.

Mean precipitation projection in the far future displays combinations of wetness and dryness both spatially and inter–seasonally over the country. Relative strength in magnitude of mean precipitation change in far future under RCP8.5 is more robust as compared to mean precipitation change in present and near future under RCP8.5 over the region. In the far future DJF season, RegCM4.3 projects relative dryness of 5 mm/day over the Northern region of the country as depicted by Figure 15. However, relative wetness of up to 4 mm/day is also projected by RegCM4.3 in the far future DJF season along the Northern belt prone to westerly systems. Moreover, relative dryness of up to 4 mm/day is also projected by RegCM4.3 in the far future DJF season over the South–eastern region of the country. In the far future MAM season, the Northern region is again projected with dryness of up to 5 mm/day while along the Northern westerly belt, a relative wetness of up to 6 mm/day is projected in the far future MAM season, as projected by RegCM4.3 under RCP8.5 scenario.

The far future JJAS season is projected by RegCM4.3 with relative dryness of up to 5 mm/day over the Northern region and with relative wetness of up to 5 mm/day over the North–eastern region of the country. Projection of relative wetness over the North–eastern region suggests strengthening of South Asian Summer Monsoon in the far future depiction by RegCM4.3. Hassan et al. (2015) reported a considerable increase of up to 2 mm/day in the precipitation over the Bay of Bengal which supports our claim of strengthening of monsoons in the projected period. However, factor of uncertainty in the projections persists in spite of numerous improvements made in the regional and global climate models since it still remains hard to explain the complexity of mechanisms that drive the variability of the Asian monsoon (Cook et al., 2010). Moreover the far future ON season is also projected by RegCM4.3 to a relative dryness of up to 4 mm/day in the Northern region of the country.

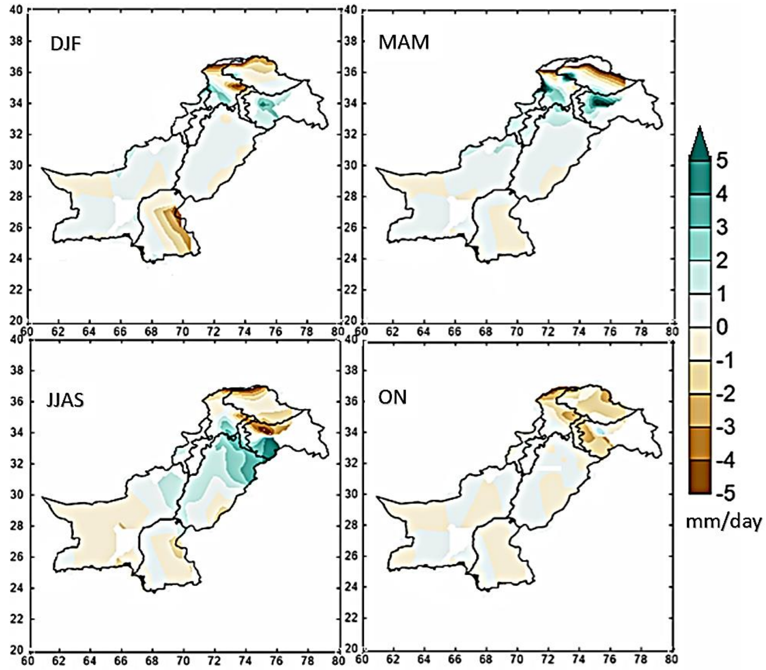

Figure 15: Projected changes (2080–2098 minus 1980–1998) in mean seasonal precipitation (mm/day) simulated by RegCM4.3.

Projected changes in temporally averaged extremes of mean temperature (°C) and mean precipitation (mm/day) for RegCM4.3 are summarized in Table 5.

Table 5: Projected changes in temporally averaged extremes of mean temperature (°C) and mean precipitation (mm/day) for RegCM4.3.

GCM20			
Time Scale	**Season**	**Δ Temperature (°C)**	**Δ Precipitation (mm/day)**
2007-2025	DJF	11	-0.4(0.6)
	MAM	8	-0.5(0.6)
	JJAS	10	-0.5
	ON	10	0.6
2080-2098	DJF	11	-5(5)
	MAM	11	-5(6)
	JJAS	11	-5(5)
	ON	11	-4

It is already seen in previous studies that systematic biases depend on the selection of parameterization schemes that have different performance gauges over different regions. The cumulus convective scheme used in the present study is Emannuel scheme (Emannuel 1991). Emannuel scheme tends to yield exaggerated precipitation over land as compared to other schemes. Previous studies have also highlighted that the simulation of South Asian summer monsoon precipitation by RegCM is sensitive to the physics parameterization used. Kar et al. (2011) and Acharya et al. (2011) also found that RegCM bears systematic biases for summer monsoon precipitation over the region. However Hassan et al. (2015) argued that RegCM4.3 reduces the temperature and precipitation biases of the driving GCM and improves the simulation results. Gao et al. (2006), Giorgi and Mearns (1999), Brankovic and Gregory

(2001) and Rauscher et al. (2010) also reported improvement in RegCM results over their respective regions.

Conclusions

Uncertainties in the projected impacts of climate change are assessed with respect to changes in long-term mean climate of both GCM20 and RegCM4.3 outputs. Future projections show substantial changes with a relatively large spread of results attributable to uncertainties in future climate expressed by the different scenarios. In contrast, our results also show how a GCM and an RCM can provide consistent climate change signal though differing in magnitude. Our results hint at both systematic and non-systematic differences between the RCM and the GCM projections of temperature and precipitation. Moreover our results caution against the use of direct GCM and RCM outputs in impact models, due to biases in the representation of present-day climate. The contribution of the different uncertainty sources vary with temporal and spatial scales.

Acknowledgements

The authors thank Goddard Institute for Space Studies (GISS NASA) for providing reanalysis datasets for this research work. Special regards to Data Integration and Analysis System (DIAS) for providing Global Circulation Model (GCM) data. The authors are grateful to International Center for Theoretical Physics (ICTP) for providing output of Regional Climate Model (RCM) simulated over Pakistan. The authors thank Pakistan Meteorological Department (PMD) for providing technical resources for this study.

References

Acharya, N., S. C. Kar, U. C. Mohanty, M. A. Kulkarni, S. K. Dash, 2011: Performance of GCMs for seasonal prediction over India−A case study for 2009 monsoon. Theoretical and Applied Climatology 105:505–520.

Ahmad, B., G. Rasul, W. Iqbal, S. A. A. Bokhari, 2014: Regional comparison between global circulation model GCM20 and regional climate model PRECIS. Pakistan Journal of Meteorology 11: 40–51.

Ahmad, B., S. Haider, and S. A. A. Bukhari, 2015: Regional precipitation response to regional warming in past and future climate. Pakistan Journal of Meteorology 11: 57–75.

Ahrens, C. D., 2000: Meteorology today: An introduction to weather, climate, and the environment. Pacific Grove, CA: Brooks/Cole Pub.

Ashfaq, A., M. Ashfaq, G. Rasul, S. A. Wajid, T. Khaliq, F. Rasul, U. Saeed, M. H. U. Rahman, J. Hussain, I. A. Baig, S. A. A. Naqvi, S. A. A. Bokhari, S. Ahmad, W. Naseem, G. Hoogenboom, 2015: Impact of climate change on the rice-wheat cropping system of Pakistan. In: Handbook of Climate Change and Agro-ecosystems, Vol. 3 (editors) Hillel D and Rosenzweig C. Imperial College Press and the American Society of Agronomy 219−258.

Brankovic, C., and D. Gregory, 2001: Impact of horizontal resolution on seasonal integrations. Climate Dynamics 18: 123−143.

Chen, J., F, P. Brissette, R. Leconte, 2011: Uncertainty of downscaling method in quantifying the impact of climate change on hydrology. Journal of Hydrology 401: 190–202, DOI: 10.1016/j.jhydrol.2011.02.020.

Cook, E. R., K. J. Anchunkaitis, B. M. Buckley, R. D. D'Arrigo, G. C. Jacoby, W. E. Wright, 2010: Asian Monsoon failure and magadrought during the last millennium. Science 328: 486–489.

Coppola, E., F. Giorgi, F. Raffaele, R. F. Franco, G. Giuliani, M. L. Pereira, A. Mamgain, L. Mariotti, G. T. Diro, and C. Torma, 2014: Present and future climatologies in the phase I CREMA experiment. Climatic Change. 125: 23–38.

Din, K., S. Tariq, A. Mahmood, G. Rasul, 2014: Temperature and Precipitation: GLOF triggering indicators in Gilgit–Baltistan, Pakistan. Pakistan Journal of Meteorology 20: 39–56.

Dunn, R. J. H., K. M. Willett, P. W. Thorne, E. V. Woolley, I. Durre, A. Dai, D. E. Parker, and R. S. Vose, 2012: HadISD: a quality controlled global synoptic report database for selected variables at long-term stations from 1973-2010. Climate of Past 8, 1649−1679.

Emannuel, K. A., 1991: A scheme for representing cumulus convection in large-scale models. Journal of Atmospheric Sciences 48: 2313–2335.

Farooqi, A. B., A. H. Khan, H. Mir, 2005: Climate change perspective in Pakistan. Pakistan Journal of Meteorology 2: 11–21.

Gao, X. J., Z. C. Zhao, Y. H. Ding, R. H. Huang, F. Giorgi, 2001: Climate change due to greenhouse effects in China as simulated by a regional climate model. Advances in Atmospheric Sciences 18: 1224–1230.

Gao, X., J. S. Pal, F. Giorgi, 2006: Projected changes in mean and extreme precipitation over the Mediterranean region from a high resolution double nested RCM simulation. Geophysical Research Letters 33 L03706.

Giorgi, F., and L. O. Mearns, 1999: Introduction to special section: Regional climate modeling revisited. Journal of Geophysical Research 104(D6): 6335−6352.

Giorgi, F., E. Coppola, F. Solmon, L. Mariotti, M. B. Sylla, X. Bi, N. Elguindi, G. T. Diro, V. Nair, G. Giuliani, U. U. Turuncoglu, S. Cozzini, I. Güttler, T. A. O'Brien, A. B. Tawfik, A. Shalaby, A. S. Zakey, A. L. Steiner, F. Stordal, L. C. Sloan, C. Brankovic, 2012: RegCM4: model description and preliminary tests over multiple CORDEX domains. Climate Research 52: 7–29, DOI: 10.3354/cr01018.

Giorgi, F., Y. Huang, K. Nishizawa, and C. Fu, 1999: A seasonal cycle simulation over eastern Asia and its sensitivity to radioactive transfer and surface processes. Journal of Geophysical Research 104: 6403–6423.

Gu, H., G. Wang, Z. Yu, R. Mei, 2012: Assessing future climate changes and extreme indicators in east and south Asia using RegCM regional climate model. Climatic Change 114: 301–317.

Hassan, M., D. Penfei, W. Iqbal, W. Can, F. Wei, W. Ba, 2014: Temperature and Precipitation Climatology Assessment over South Asia using the Regional Climate Model (RegCM4.3): An Evaluation of the Model Performance. Journal of Earth Sciences and Climatic Change 5: 214. DOI: 10.4172/2157–7617.1000214.

Hassan, M., D. Pengfei, J. Shaofeng, I. Waheed, M. Rashid, and B. Wulong, 2015: An assessment of the south Asian summer monsoon variability for present and future climatologies using a high resolution regional climate model (RegCM4.3) under the AR5 scenarios. Atmosphere 6: 1833–1857 doi:10.3390/atmos6111833.

Iwami, Y., H. Akira, M. Mamoru, K. Shun, Y. Yusuke, U. Tomoki, K. Toshio, 2017: Comparative study on climate change impact on precipitation and floods in Asian river basins. Hydrological Research Letters 11: 24–30, DOI: 10.3178/hrl.11.24.

Janjua, P. Z., G. Samad, N. U. Khan, 2010: Impact of climate change on wheat production: A case study of Pakistan. The Pakistan Development Review 49: 799–822.

Kalim, U., S.T. Gao, 2012: Moisture transport over the Arabian associated with the summer rainfall over Pakistan in 1994 and 2002. Advances in Atmospheric Sciences 29: 501 –508.

Kar, S. C., N. Acharya, U. C. Mohanty, M. A. Kulkarni, 2011: Skill of monthly rainfall forecasts over India using multi-model ensemble schemes. International Journal of Climatology 32: 1271-1286.

Kazmi, D. H., J. Li, G. Rasul, J. Tong, G. Ali, S. B. Cheema, L. Liu, M. Gemmer, T. Fischer, 2014: Statistical downscaling and future scenario generation of temperature for Pakistan regions. Theoretical and Applied Climatology 120: 341–350.

Kumar, A., A. Wiltshire, C. Mathison, S. Asharaf, B. Ahrens, P. Lucas-Picher, J. H. Christensen, A. Gobiet, F. Saeed, S. Hagemann, 2013: Downscaled climate change projections with uncertainty assessment over India using a high resolution multi-model approach. Science of the Total Environment 468–469: S18–S30.

Kusunoki, S., J. Yoshimura, H. Yoshimura, A. Noda, 2006: Change of baiu rain band in global warming projection by an atmospheric general circulation model with a 20-km grid size. Journal of the Meteorological Society of Japan 84: 581–611.

M. A. Rouf, M. K. Uddin, S. K. Debsarma, M. M. Rahman, 2011: Climate of Bangladesh: An analysis of northwestern and southwestern part using high resolution Atmosphere-Ocean General Circulation Model (AOGCM) The Agriculturists 9: 143-154.

Mamgain, A., M. Laura, C. Erika, G. Filippo, and K. D. Sushil, 2013: Sensitivity of RegCM4.3 two convection schemes on Indian summer monsoon for the South Asia CORDEX domain. Geophysical Research Abstracts 15: 4812.

Minville, M., F. Brissette, R. Leconte, 2008: Uncertainty of the impact of climate change on the hydrology of a nordic watershed. Journal of Hydrology 358: 70–83, DOI: 10.1016/j.jhydrol.2008.05.033.

Mizuta, R., H. Yoshimura, H. Murakami, M. Matsueda, H. Endo, T. Ose, K. Kamiguchi, M. Hosaka, M. Sugi, S. Yukimoto, S. Kusunoki , A. Kitoh, 2012: Climate simulations using MRI-AGCM3.2 with 20-km grid. Journal of the Meteorological Society of Japan 90A: 233–258.

Ozturk, T., H. Altinsoy, M. Türkeş, M. Kurnaz, 2012: Simulation of temperature and precipitation climatology for the Central Asia CORDEX domain using RegCM 4.0. Climate Research 52: 63–76, DOI: 10.3354/cr01082.

Raju, A., A. Parekh, J.S. Chowdary, C. Gnanaseelan, 2015: Assessment of the Indian summer monsoon in the WRF regional climate model. Climate Dynamics 44: 3077–3100.

Rasul, G., M. Afzal, M. Zahid, S. A. A. Bukhari, 2012: Climate change in Pakistan focused on Sindh province. Technical Report No. PMD-25/2012.

Rauscher, S. A, E. Coppola, C. Piani, F. Giorgi, 2010: Resolution effects on regional climate model simulations of seasonal precipitation over Europe. Climate Dynamics 35: 685−711.

Ruane, A., R. Goldberg, J. Chryssanthacopoulos, 2014: AgMIP climate forcing datasets for agricultural modeling: Merged products for gap–filling and historical climate series estimation. Agricultural and Forest Meteorology 200: 233–248, DOI:10.1016/j.agrformet.2014.09.016.

Salathe, J. E. P., 2004: Methods for selecting and downscaling simulations of future global climate with application to hydrologic modelling. International Journal of Climatology 25: 419–436.

Shakoor, U., A. Saboor, I. Ali, A. Mohsin, 2011: Impact of climate change on agriculture: Empirical evidence from arid region. Pakistan Journal of Agricultural Sciences 48: 327–333.

Syed, F.S., W. Iqbal, S. A. A. Bokhari, and G. Rasul, 2014: Uncertainties in the regional climate models simulations of South–Asian summer monsoon and climate change. Climate Dynamics 42: 2079–2097.

Tatsumi, K., Y. Yamashiki, K. Takara, E. Nakakita, 2013: Reproducibility of Crop Yield Simulated by iGAEZ Model with High-resolution GCM Output. Journal of Agricultural Science and Applications 2: 124–130, DOI: 10.14511/jasa.2013.020211.

Tisseuil, C., M. Vrac, S. Lek, A. J. Wade, 2010: Statistical downscaling of river flows. Journal of Hydrology 385: 279–291, DOI: 10.1016/j.jhydrol.2010.02.030.

Winkler, J. A., G. S. Guentchev, M. Liszewska, P. Tan, 2011: Climate scenario development and applications for local ⁄ regional climate change impact assessments: An overview for the non–climate scientist part II : considerations when using climate change scenarios. Geography Compass 6: 301–328.

Wood, A., L. R. Leung, V. Sridhar, D. P. Lettenmaier, 2004: Hydrologic implications of dynamical and statistical approaches to downscaling climate model outputs. Climatic Change 62:189–216.